CANCER BIOTHERAPY & RADIOPHARMACEUTICALS
Volume 22, Number 3, 2007

DOI: 10.1089/cbr.2007.347

Single-Cell Dosimetry for Radioimmunotherapy of B-Cell Lymphoma Patients with Special Reference to Leukemic Spread

Cecilia Hindorf,[1] Dimitris Emfietzoglou,[2] Ola Lindén,[3] Christos Bousis,[2] Andreas Fotopoulos,[4] Kostas Kostarelos,[5] and Glenn D. Flux[1]
[1]Joint Department of Physics, Institute of Cancer Research and Royal Marsden NHS Foundation Trust, Sutton, Surrey, United Kingdom
[2]Department of Medical Physics, University of Ioannina Medical School, Ioannina, Greece
[3]Department of Oncology, Lund University Hospital, Lund, Sweden
[4]Department of Nuclear Medicine, University Hospital of Ioannina, Ioannina, Greece
[5]Centre for Drug Delivery Research, The School of Pharmacy, University of London, United Kingdom

ABSTRACT

Aims: *Many lymphoma patients have both macroscopic tumors and single-cell manifestations of their disease. Treatment efficacy could, therefore, depend on the radionuclide used. The aim of this study was to investigate dosimetry at a cellular level for three isotopes of radioiodine.* ***Methods:*** *Cells were assumed to be spherical with radii of 6.35, 7.7, and 9.05 μm corresponding to the dimensions of the Raji cells. The radius of the nucleus was assumed to be 75% of the cellular radius. The electron energies were 18, 28, and 190 keV, corresponding to the mean electron energy per decay for ^{125}I, ^{123}I, and ^{131}I, respectively. S-values for different activity distributions were simulated using Monte Carlo and dose-volume histograms as well as absorbed doses, and absorbed dose rates were calculated.* ***Results:*** *^{125}I gives the highest absorbed dose (~4–40 times that of ^{131}I), whereas ^{123}I will give the highest absorbed dose rate (~100 times that of ^{131}I). Under the given assumptions, the absorbed dose at this level is more dependent on the size of the cells than on whether the radioimmunoconjugate is internalized.* ***Conclusions:*** *This enquiry showed that both ^{123}I and ^{125}I have greater potential than ^{131}I for the treatment of leukemic spread in patients with lymphoma.*

Key words: dosimetry, lymphoma, single cells

INTRODUCTION

Radioimmunotherapy (RIT) for lymphoma is presently optimized for treating macroscopic tumors. However, many patients have microscopic disease and virtually all patients diagnosed with the most common type of lymphoma, chronic lymphocytic leukemia (CLL), have many single tumor cells circulating in the blood. The latter group makes up approximately 25% of all diagnosed lymphomas.[1] The tumor manifestations in the very same lymphoma patient can range in size from more than one liter down to the volume of one single cell.

Address reprint requests to: Cecilia Hindorf; Joint Department of Physics, Institute of Cancer Research and Royal Marsden NHS Foundation Trust; Sutton, Surrey SM2 5PT United Kingdom; Tel.: +44 (0)208 661 3288; Fax: +44 (0)208 643 3812
E-mail: **cecilia.hindorf@icr.ac.uk**

RIT for lymphoma is presently optimized for treating macroscopic tumors. However, many patients have microscopic disease or disease only assessable by polymerase chain reaction (PCR). Patients diagnosed with the most common type of lymphoma, CLL, have, by definition, disease involvement of the blood and a lymphocyte count larger than 10×10^9 (although a diagnosis of CLL is possible with a number of lymphocytes less than 10×10^9).[2] CLL makes up approximately 25% of all diagnosed lymphomas.[1] The tumor manifestations in the very same lymphoma patient can thus range in size from a single cell to up to masses of more than 5 cm in diameter.

There are two Food and Drug Administration (FDA)-approved radiopharmaceuticals for the treatment of lymphoma, Zevalin and Bexxar. Zevalin uses an antibody labeled with ^{90}Y and a long-range electron-emitter (maximum beta energy of 2.28 MeV, with a maximum range in water of 11 mm) whereas Bexxar, an antibody labeled with ^{131}I, is a medium–range electron-emitter (maximum beta energy of 0.606 MeV, with a maximum range in water of 2.3 mm). Previous theoretic studies have shown the existence of an optimal relationship between electron range, tumor radius, and tumour control probability,[3,4] (i.e., not only large tumors, but also smaller tumor deposits have a lower probability of becoming eradicated). A clinical observation compatible with this notion is the report by Kaminski et al.[5] that relapse often solely occurs in sites that are not previously known to have a lymphoma involvement. Interestingly, a highly significant difference in remission rate between rituximab and Zevalin did not translate into a difference in time-to-treatment failure,[6] as might have been expected based on the correlation between response and the duration of response in the pivotal study of rituximab.[7] The high energy of β-particles from ^{90}Y and ^{131}I make them less suitable for the treatment of single cells, and the reported conversion of PCR positivity to PCR negativity following RIT may be a result of mechanisms of action other than targeted RIT.[8]

The shorter the electron range, the more important the uptake pattern is on a cellular level for delivering the cell a lethal absorbed dose. There exist two groups of monoclonal antibodies (MAbs) considering the cellular spatial distribution: non- and internalizing MAbs. A noninternalizing MAb binds to the receptors on the cell surface and stays there, where an internalizing MAb is transferred into the cell cytoplasm, the lysosomes, after binding to the receptors on the cell surface. The CD20-targeting MAbs used in Zevalin and Bexxar are both examples of noninternalizing MAbs (ibritumomab in the case of Zevalin and tositumomab in the case of Bexxar).[9] An example of an internalizing MAb for lymphomas is the humanized CD22-targeting epratuzumab (hLL2).[10]

Therefore, the aim of this study was an enquiry into single-cell dosimetry, which is necessary for the optimization of RIT targeting of single cells or small deposits of lymphoma. The Medical Internal Radiation Dose (MIRD) scheme[11,12] with Monte Carlo–evaluated S-values (the absorbed dose to the target per decay in the source) in combination with a realistic kinetic distribution on a cellular level of a radioimmunoconjugate, was applied to calculate the absorbed dose and the absorbed dose rate, which were the parameters that served as a basis for a development of the current RIT of lymphoma patients. This is the first time, to the authors' knowledge, that single-cell dosimetry, including subcellular pharmacokinetics, has been applied to clinically relevant data.

METHODS

Generation of Cellular S-Values and Dose Volume Histograms

The characteristics of single lymphoma B-cells circulating in the blood were assumed to equal the ones for Raji cells, which is a cell line commonly used as a model for lymphomas. All cells were assumed to be spherical, with radii of 6.35, 7.7, and 9.05 μm, which corresponds to the size of a Raji cell, which measures 7.7 ± 1.35 μm.[13] The radius of the cellular nucleus was assumed to be 75% of the cellular radius for all cell sizes. Either the whole cell, cell surface, or the cytoplasm was considered as source regions for the decays. The later two configurations were chosen to mimic either a noninternalizing radioimmunoconjugate, uniformly distributed on the cellular surface or an internalizing radioimmunoconjugate, uniformly distributed in the cytoplasm. Two target regions were considered, either the whole cell or the cellular nucleus. Electrons of initial energies (18, 28, and 190 keV) were used in Monte Carlo simulations. These three electron energies correspond to the mean electron energy per decay for three iodine radionuclides (18 keV for ^{125}I, 28 keV for ^{123}I, and

190 keV for ^{131}I). The mean electron energy per decay were calculated as the sum of all the emitted electron energies weighted by their probability of emissions. Details on the characteristics of the radionuclides can be seen in Table 1. Emitted photons were neglected for the dosimetry on the cellular level.

The Monte Carlo code MC4[14,15] was used for simulating stochastic tracks of electrons with initial energies of 18, 28, and 190 keV in a unit density water medium. Calculations have been performed over ~10,000 primary electrons. The statistical uncertainty of the mean values was estimated to be of less than a few percent. The point of origin for each primary electron was distributed randomly (proportional to the volume mass) inside the cell (uniform distribution), the cell cytoplasm, or the cell surface. To keep computational time at practical levels the detailed (event-by-event) simulation scheme was restricted to electrons with kinetic energies below 10 keV, whereas a condensed-history scheme was employed at higher energies. All electrons (primary and secondaries) were followed down to threshold (~10 eV). A discussion of the cross-section input with an emphasis on recent developments is provided elsewhere.[16,17] The condensed history scheme employed simulates elastic collisions in a detailed manner, according to their total and differential cross-sections, whereas energy losses between elastic events are given by the unrestricted stopping power and the continuous slowing down approximation (csda). By this method, the stochastics of angular deflection are still largely preserved, providing a somewhat realistic approximation of the spread-out pattern of the track. Because the csda scheme ignores the finite range of energetic secondaries (δ-rays) that may be capable of escaping the cell volume, we have also implemented a mixed-transport scheme to test this effect. That is, in the condensed-history domain (>10 keV), the production of hard secondaries with energies above 1 keV was individually simulated according to total and differential cross-sections, whereas a restricted-csda scheme was used for the soft energy loss events. The influence of those δ-rays to our results was found to be noticable (~5%–10%) only in the 190-keV case and the smallest cell volumes examined. As will become apparent in the Results section below, this level of discrepancy has no impact on the conclusions of this work. Thus, owing to the much higher running times required for the mixed transport scheme, the simpler csda scheme was chosen as above 10 keV.

MC4 in its hybrid scheme was used to generate S-values, S(target ← source) and dose volume histograms (DVHs) for three cell radii (6.35, 7.7, and 9.05 μm), six target ← source combinations (C [cell] ← C, C ← CS [cell surface], C ← CY [cytoplasm], N ← C, N [cell nucleus] ← CS and N ← CY), and three electron energies (18, 28, and 190 keV). For benchmarking the application of our code to the present problem, we performed simulations for electrons of 1, 10, 100, and 200 keV for spheres of a 5- and 10-μm radius and obtained S(C ← C) values that differed by only a few percent from those provided by the MIRD Committee.[18]

Dosimetry for Single-Tumor B-Cells

The self-absorbed dose and the self-absorbed dose rate were calculated for single B-cells. The MIRD scheme was applied. The cumulated activity for a B-cell was calculated assuming different kinetics for both non- and internalizing MAbs. The noninternalizing radioimmunoconjugate was assumed to bind to the receptors immediately after the administration and remained

Table 1. Radionuclide Data for ^{123}I, ^{125}I, and ^{131}I

	^{123}I	^{125}I	^{131}I
Half-life	13.1 hours	60 days	8.1 days
Mean electron energy per decay	28 keV	18 keV	190 keV
Electron range in water (μm)	16 μm	7 μm	0.4 mm
Main photon energy (abundance)	159 keV (83%)	27 keV (73%)	364 keV (81%)
Total emitted energy per decay	199 keV	58.7 keV	571 keV
Fraction of total emitted energy that is emitted by electrons	0.13	0.29	0.33

bound. One hundred and twenty-eight thousand (128,000) receptors were assumed to be present on each cell surface.[19] The internalizing radioimmunoconjugate was assumed to be internalized at a rate of 10 millions of receptors during the first 24 hours after injection.[20] It was also assumed that the iodine stayed in the cell once it was internalized, which is a reasonable assumption for a residualizing radiolabel.[21] For noninternalizing MAbs, S-values with the cell surface as the source were used (S[C ← CS], S[N ← CS]) and for internalizing with both the cell and the cytoplasm as the sources (S[C ← C], S[N ← C] and S[C ← CY], S[N ← CY]).

The specific activities (number of atoms per MAb) for the radioimmunoconjugates were recalculated from the specific activity for the residualizing labeling method for ^{125}I developed by Govindan et al. (0.76 atoms/Mab).[22] This corresponds to 45 GBq/mg MAb for ^{123}I, 410 MBq/mg MAb for ^{125}I, and 3 GBq/mg MAb for ^{131}I. All available binding sites at the cellular surface were assumed to be saturated, which has been shown to be true *in vivo* for $CD19^-$.[23]

The cross-absorbed dose to blood circulating single B-cells was estimated by calculating the mean absorbed dose to the blood under an assumption of a uniform spatial distribution of the activity in the blood. The absorbed dose to the blood was estimated by assuming the total radiation equilibrium (emitted energy equals absorbed energy at any point in space). The maximum activity concentration in the blood was calculated based on the number of B-cells in the blood, the number of receptors on the cell surface, and the specific activity of the radiopharmaceutical.

Whole-Body Dosimetry

The MIRD scheme was applied for whole-body dosimetry. A maximum activity present in the whole body was calculated based on the maximum uptake to each B-cell and the total number of B-cells in the body ($1*10^7$ B-cells/mL of blood, with a total blood volume of 5 L). However, the absorbed dose to the whole body was constrained to be equal to or less than 0.5 Gy, and the maximum activity to administer for all the radiopharmaceuticals was based on this constraint. Human MAbs circulating in the blood have a biologic half-life of approximately 3 weeks. However, because it was assumed that all MAbs did bind to tumor cells, no biologic clearance of the radiopharmaceutical (only the physical decay of the radionuclide) was assumed. S-values for the adult male phantom were taken from the RADAR website (www.doseinfo-radar.com/RADARphan.html).[24]

RESULTS

Absorbed fractions and S-values for the three electron energies/iodine radionuclides (18 keV/^{125}I, 28 keV/^{123}I, and 190 keV/^{131}I) can be seen in Table 2 for six target ← source configurations (C ← C, C ← CS, C ← CY, N ← C, N ← CS, and N ← CY) and three cellular radii (6.35, 7.7, and 9.05 μm). The S-value for a source distribution on the cell surface is always less than if the source is distributed in the cytoplasm. The S-values decrease with an increase in both cell size and electron energy. Because the above combination of energies and cell dimensions are not included in the MIRD cellular S-value tabulation,[18] we also performed analytic calculations of S-values based on Cole's energy-range formula following the MIRD methodology.[18] Deviations between the Monte Carlo and analytic calculations were less than 10% at 18 and 190 keV, and reached up to 20% at 28 keV (the largest discrepancies being found when the nucleus was the target).

Figure 1 shows the effect of cell size on the differential DVHs for a uniform activity distribution in a cell with a radius of 7.7 μm for the three electron energies. The importance of the cell size increases as the electron energy decreases. A small cell has a higher mean value of the absorbed dose than a larger cell, but the distribution is wider. Also, with decreasing electron energy, the mean value and the width of the distribution both increase. The effects of different activity distributions in the cell on the differential DVH is shown in Figure 2. The subcellular distribution of the activity is not important for the 190-keV electrons. For 18- and 28-keV electrons, the distribution in the absorbed dose is narrower for activity in the cytoplasm than for activity distributed in the cell and at the cell surface. In particular, with decreasing electron energy, the spatial distribution of activity has a higher impact on the distribution of absorbed dose within the cell volume.

The administered activity required to deliver an absorbed dose to the whole body of 0.5 Gy was calculated to be 33 GBq for ^{123}I, 590 MBq for ^{125}I, and 700 MBq for ^{131}I.

Table 2A. Absorbed Fractions and S-Values for the Whole Cell as Target-Region and the Cell (C ← C), Cell Surface (C ← CS), and Cytoplasm (C ← CY) as Source-Regions for Three Electron Energies (18, 28, and 190 keV) and Three Cell Radii (6.35, 7.7, and 9.05 μm)

Electron energy (keV)	*Cell radius (μm)*	*Absorbed fraction (AF)*			*S-value (mGy/Bq s)*		
		AF(C ← C)	*AF(C ← CS)*	*AF(C ← CY)*	*S(C ← C)*	*S(C ← S)*	*S(C ← CY)*
18	6.35	0.52	0.34	0.44	1.407	0.914	1.193
	7.7	0.60	0.37	0.49	0.897	0.554	0.745
	9.05	0.67	0.40	0.54	0.617	0.369	0.504
28	6.35	0.21	0.14	0.19	0.860	0.589	0.778
	7.7	0.27	0.20	0.25	0.627	0.463	0.576
	9.05	0.34	0.23	0.31	0.492	0.334	0.442
190	6.35	0.0069	0.0046	0.0060	0.196	0.130	0.170
	7.7	0.0085	0.0057	0.0074	0.135	0.090	0.118
	9.05	0.0099	0.0066	0.0087	0.097	0.065	0.085

Table 2B. Absorbed Fractions and S-Values for the Cell Nucleus as Target-Region and the Cell (N ← C), Cell Surface (N ← CS), and Cytoplasm (N ← CY) as Source-Regions for Three Electron Energies (18, 28, and 190 keV) and Three Cell Radii (6.35, 7.7, and 9.05 μm)

Electron energy (keV)	*Cell radius (μm)*	*Absorbed fraction (AF)*			*S-value (mGy/Bq s)*		
		AF(N ← C)	*AF(N ← CS)*	*AF(N ← CY)*	*S(N ← C)*	*S(N ← S)*	*S(N ← CY)*
18	6.35	0.28	0.12	0.18	1.785	0.793	1.160
	7.7	0.30	0.13	0.19	1.082	0.461	0.682
	9.05	0.35	0.13	0.20	0.769	0.275	0.433
28	6.35	0.098	0.046	0.067	0.967	0.453	0.662
	7.7	0.130	0.066	0.088	0.719	0.365	0.487
	9.05	0.165	0.085	0.116	0.563	0.290	0.399
190	6.35	0.0034	0.0016	0.0021	0.228	0.108	0.1386
	7.7	0.0042	0.0019	0.0027	0.157	0.0714	0.0999
	9.05	0.0048	0.0023	0.0030	0.112	0.0532	0.0694

The self-absorbed dose to a cell and a cell nucleus when the injected activity is restricted to give a maximal absorbed dose to the whole body of 0.5 Gy for non- and internalizing MAbs, as well as the maximal self-absorbed dose, is presented in Table 3. The highest absorbed dose to both the cell and the cell nucleus is delivered by ^{125}I and the lowest by ^{131}I for all source distributions, except for the case of ^{125}I distributed on the cell surface of the largest cell radius (9.05 μm). The mean absorbed dose on a cellular level is always constrained by the maximal absorbed dose to the whole body. The absorbed dose for an internalizing MAb and ^{123}I is limited by the combination of the uptake phase of the radiopharmaceutical and the very short physical half-life (13 hours). The ratio of the maximal absorbed dose for an internalizing MAb and a noninternalizing MAb is approximately 100 for the three radionuclides and is a result of the limited number of receptors on the cell surface. There is an accumulation process of the internalizing MAb within the cell that is not present for a noninternalizing MAb. The size of the cross-absorbed dose was estimated to be negligible, compared to the self-absorbed dose ($<1*10^{-4}$ of the self-absorbed dose).

The absorbed dose rate depends on both the energy of emitted electrons and the half-life of the radionuclide (if the pharmacokinetics are assumed to be the same), which make the patterns of the absorbed dose rates as a function of time for the three iodine isotopes differ significantly, as can be seen in Figure 3. The maximum absorbed dose rate to the cell for a uniform activity distribution in the cell differs by nearly two orders of magnitude, with the lowest being for ^{131}I (0.006 Gy/hour) and the highest being for

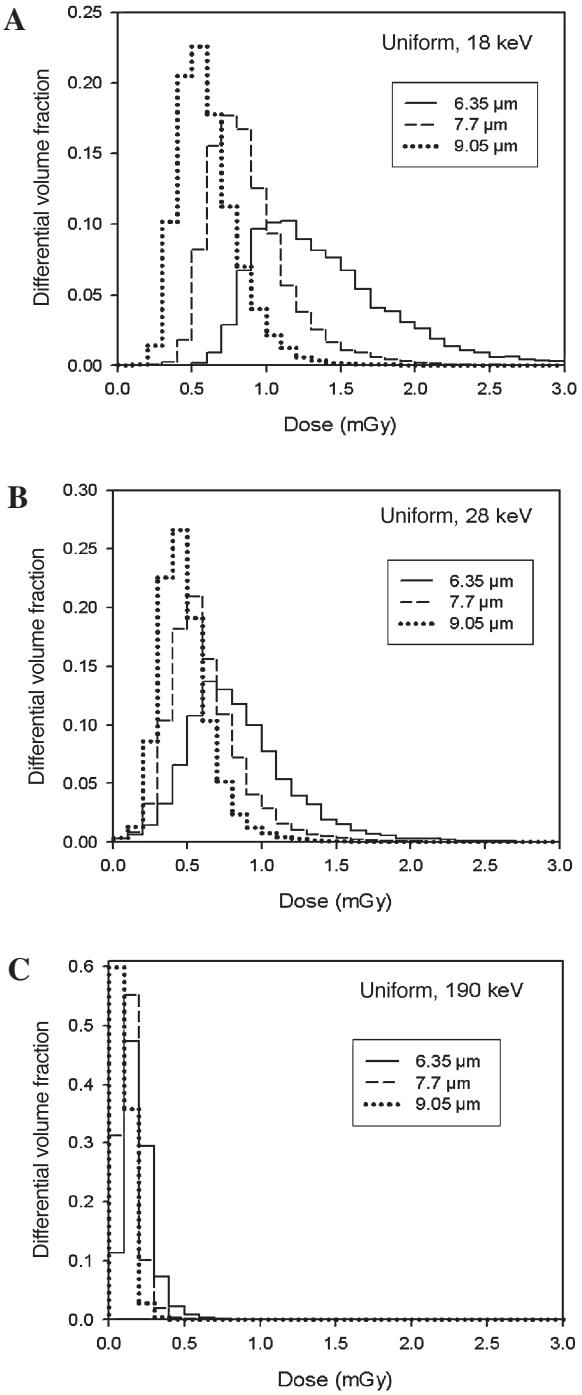

Figure 1. Differential dose-volume histograms for a uniform activity distribution in the cell for three cellular radii (**A**) 6.35 μm; (**B**) 7.7 μm; (**C**) 9.05 μm for three monoenergetic electron energies (18, 28, and 190 keV).

^{123}I (0.24 Gy/hour) when the administered activity is constrained by the whole-body absorbed dose. The self-absorbed dose rate in the cell nucleus as a function of time following an administration of an internalized, surface-bound radioimmunoconjugate labeled to ^{123}I, ^{125}I, and ^{131}I is presented in Figure 4. The absorbed dose rate on the cellular level in Figure 4 is based on an administered activity that gives a maximal absorbed dose of 0.5 Gy to the whole body.

DISCUSSION

In all the experimental studies that we are aware of, Auger emitters were therapeutically superior to β-emitters when taken to the maximum tolerated activity (MTA).[25–27] One of the Auger emitters that more easily may be taken to the clinic is ^{125}I, which is easy to label and also has the theoretic advantage of having a comparably high percentage of its energy emitted as electrons. In this work, the single absorbed dose from ^{125}I was compared to the one from ^{123}I and ^{131}I, which is a label used for RIT. It may be possible to give a significantly higher activity/absorbed dose with ^{125}I than ^{131}I, which is indicated by a study in which the MTA was not reached at 13 GBq/m^2.[28] Interestingly, in an experimental model, the MTA was 10 times higher for ^{125}I than for ^{131}I.[25]

This study showed that ^{125}I-labeled MAbs give a higher absorbed dose on a cellular level than ^{123}I and ^{131}I. The absorbed dose received from a noninternalizing MAb for ^{125}I is approximately a factor of two greater than the absorbed dose for ^{123}I (Table 3) when the administered activity is restricted by the whole-body absorbed dose of 0.5 Gy. However, the absorbed dose rate is nearly a magnitude greater for ^{123}I than for ^{125}I (Fig. 3). Even if there were an approximate 10-fold difference in dose rate, the importance of it would be unclear. On the contrary, a clear relationship between administered activity and response in terms of survival has been shown in an animal model of RIT of B-cell lymphoma.[29]

The DVHs in Figure 2 show that the choice of combination of electron energy and internalizing or noninternalizing radioimmunoconjugate only is of importance for the lower electron energies (18 and 28 keV). When the injected activity is restricted by a fixed whole-body absorbed dose, these calculations show that the absorbed dose to a cell or cell nucleus from ^{123}I, unlike that from ^{125}I and ^{113}I, depends on whether the antibody is internalized (Table 3). If the injected activity could be increased, that is, if it is not restricted by bone marrow toxicity or it may be circumvented by stem-cell support, the results in Table 3 show that

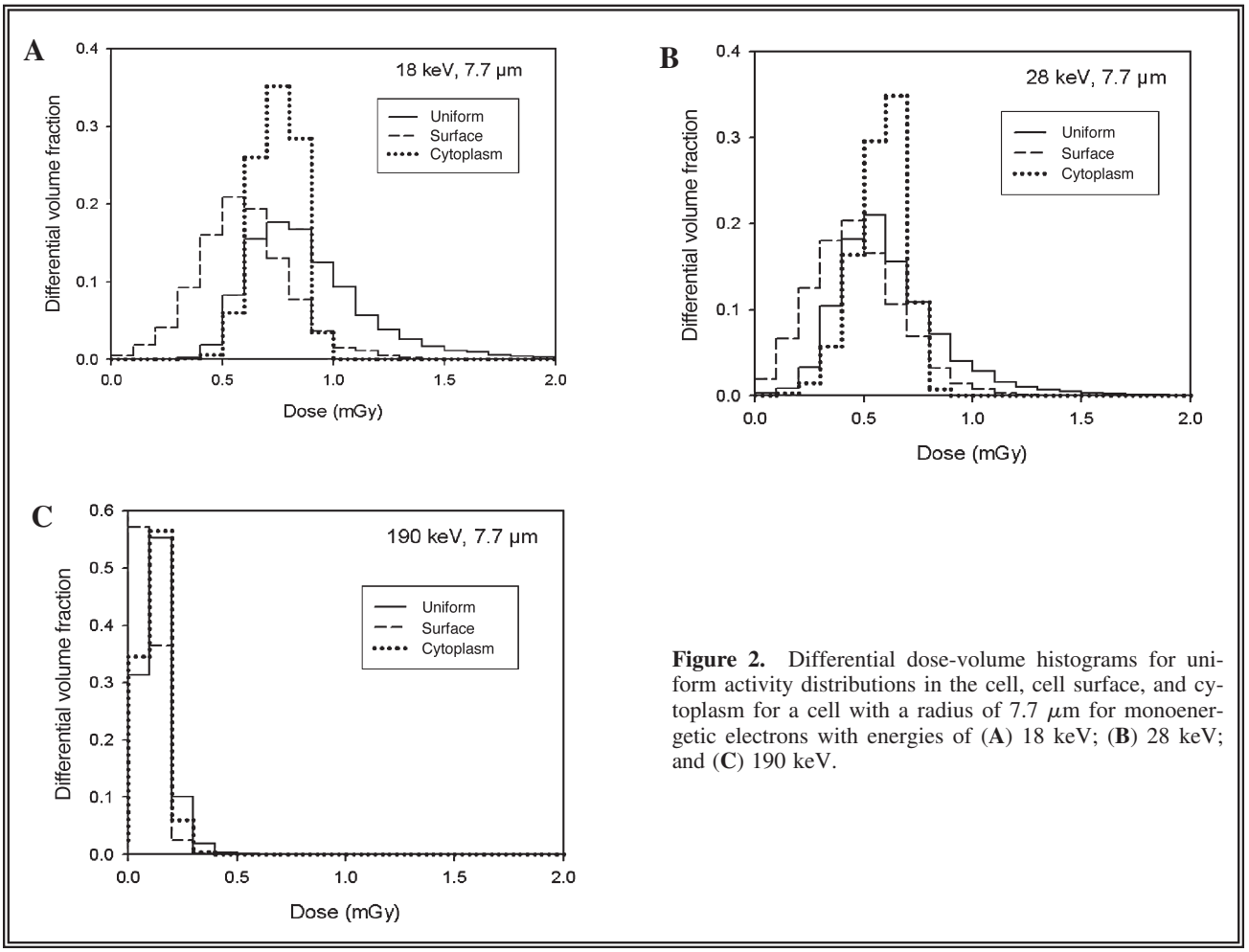

Figure 2. Differential dose-volume histograms for uniform activity distributions in the cell, cell surface, and cytoplasm for a cell with a radius of 7.7 μm for monoenergetic electrons with energies of (**A**) 18 keV; (**B**) 28 keV; and (**C**) 190 keV.

Table 3. Mean and Maximum Absorbed Dose to the Cell and Nucleus from Activity Uniformly Distributed in the Cell, Cytoplasm, and on the Cell Surface for Three Cell Radii (6.35 and Three Radionuclides, (^{123}I, ^{125}I, and ^{131}I)

	Cell radius (μm)	*^{123}I (mean)*	*^{123}I (max)*	*^{125}I (mean)*	*^{125}I (max)*	*^{131}I (mean)*	*^{131}I (max)*
D(C ← C)	6.35	9.0E + 00	5.4E + 03	1.0E + 02	8.9E + 03	2.4E + 00	1.4E + 03
(Gy)	7.70	6.6E + 00	4.0E + 03	6.5E + 01	5.7E + 03	1.7E + 00	9.9E + 02
	9.05	5.1E + 00	3.1E + 03	4.5E + 01	3.9E + 03	1.2E + 00	7.1E + 02
D(C ← CY)	6.35	8.1E + 00	4.9E + 03	8.6E + 01	7.5E + 03	2.1E + 00	1.3E + 03
(Gy)	7.70	6.0E + 00	3.6E + 03	5.4E + 01	4.7E + 03	1.4E + 00	8.7E + 02
	9.05	4.6E + 00	2.8E + 03	3.6E + 01	3.2E + 03	1.0E + 00	6.2E + 02
D(C ← CS)	6.35	2.6E + 01	5.8E + 01	8.1E + 01	8.9E + 01	1.8E + 00	1.3E + 01
(Gy)	7.70	2.1E + 01	4.5E + 01	4.9E + 01	5.4E + 01	1.3E + 00	8.8E + 00
	9.05	1.5E + 01	3.3E + 01	3.3E + 01	3.6E + 01	9.0E − 01	6.4E + 00
D(N ← C)	6.35	1.0E + 01	6.1E + 03	1.3E + 02	1.1E + 04	2.8E + 00	1.7E + 03
(Gy)	7.70	7.5E + 00	4.5E + 03	7.8E + 01	6.8E + 03	1.9E + 00	1.2E + 03
	9.05	5.9E + 00	3.6E + 03	5.6E + 01	4.9E + 03	1.4E + 00	8.2E + 02
D(N ← CY)	6.35	6.9E + 00	4.2E + 03	8.4E + 01	7.3E + 03	1.7E + 00	1.0E + 03
(Gy)	7.70	5.1E + 00	3.1E + 03	4.9E + 01	4.3E + 03	1.2E + 00	7.3E + 02
	9.05	4.2E + 00	2.5E + 03	3.1E + 01	2.7E + 03	9.0E − 01	5.1E + 02
D(N ← CS)	6.35	2.0E + 01	4.4E + 01	7.0E + 01	7.8E + 01	1.5E + 00	1.1E + 01
(Gy)	7.70	1.6E + 01	3.6E + 01	4.1E + 01	4.5E + 01	1.0E + 00	7.0E + 00
	9.05	1.3E + 01	2.8E + 01	2.4E + 01	2.7E + 01	7.0E − 01	5.2E + 00

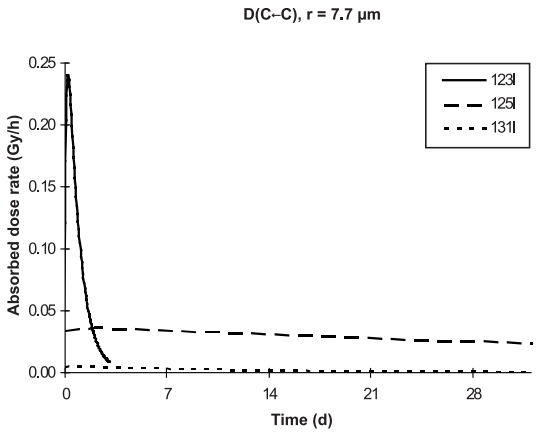

Figure 3. Absorbed dose rate to a cell from activity uniformly distributed in the cell (radius, 7.7 μm) as a function of time following the administration of three iodine isotopes (^{123}I, ^{125}I, and ^{131}I). The administered activities were constrained by a whole-body absorbed dose of 0.5 Gy.

the use of an internalizing MAb is superior to a noninternalizing MAb, assuming the high number of internalized antibodies. These calculations also show that an increase in specific activity may be of more importance for a noninternalizing MAb, as the number of receptors on the cell surface otherwise would limit the absorbed dose. This is of a particular interest if the patient has a very low receptor expression per cell. The number of radiolabeled MAbs in the cytoplasm of each cell for an internalizing radioimmunoconjugate would be quite high, even with a low receptor expression on the cell surface and it is more likely that the injected activity is limiting the uptake on the cellular level. The maximum absorbed dose per cell is very dependent on a high specific activity, whereas the mean absorbed dose is limited by the administered activity.

In this work, a number of assumptions were made. First, the receptors on the cell surface and

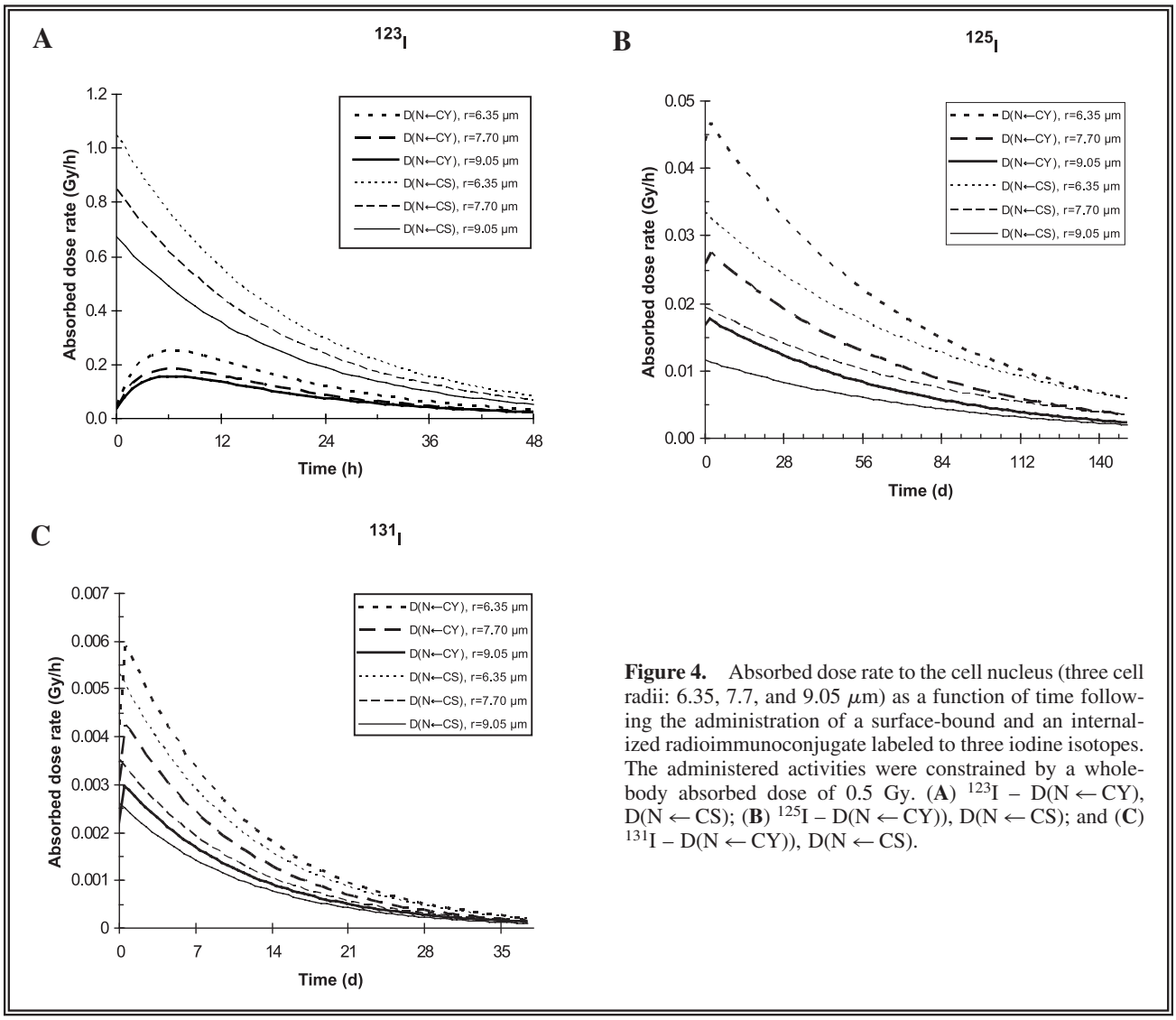

Figure 4. Absorbed dose rate to the cell nucleus (three cell radii: 6.35, 7.7, and 9.05 μm) as a function of time following the administration of a surface-bound and an internalized radioimmunoconjugate labeled to three iodine isotopes. The administered activities were constrained by a whole-body absorbed dose of 0.5 Gy. (**A**) ^{123}I – D(N ← CY), D(N ← CS); (**B**) ^{125}I – D(N ← CY)), D(N ← CS); and (**C**) ^{131}I – D(N ← CY)), D(N ← CS).

the amount of internalization of the radioimmunoconjugate were assumed to not vary with the cellular size, which had the consequence that larger cells may have had a somewhat false low absorbed dose for a given radionuclide. Furthermore, the presumed number of cell-surface receptors for non-internalized antibodies was not overestimated but may be somewhat low, in view of what has been published for CD52.[30] The distribution of cell sizes in a patient would probably be larger, assuming a patient had follicular lymphoma, than for Raji cells, which we used as a basis for these calculations; also, for each cell size, there would be a distribution of the size of the nucleus, which also would affect the absorbed dose. Finally, all S-values were simulated with the cell nucleus at the center of the cell, which is often not true for a B-cell, which often would have its nucleus paracentrally located.

CONCLUSIONS

This study showed that ^{131}I, the iodine isotope that is currently the most widely used for RIT, gave the lowest absorbed dose and absorbed dose rate on a cellular level of the iodine isotopes that were investigated. ^{125}I gave the highest absorbed dose, whereas ^{123}I gave the highest absorbed dose rate. The maximal absorbed dose to a cell would be restricted by the whole-body absorbed dose (and thus by the administered activity). Internalizing antibodies are better combined with ^{125}I with its longer half-life.

REFERENCES

1. Johnson A, Cavallin-Ståhl E, Åkerman M. Flow cytometric light-chain analysis of peripheral blood lymphocytes in patients with non-Hodgkin's lymphoma. *Br J Cancer* 1985;52:159.
2. Muller-Hermelink HK, Montserrat E, Catovsky D, et al. Chronic lymphocytic leukaemia/small lymphocytic lymphoma. In: Jaffe ES, Harris NL, Stein H, Vardiman JW, eds. *Tumours of the Haematopoietic and Lymphoid Tissues.* Lyon, United Kingdom: IARC Press, 2001.
3. Nahum AE. Microdosimetry and radiocurability: Modelling targeted therapy with beta-emitters. *Phys Med Biol* 1996;41:1957.
4. O'Donoghue JA, Bardiès M, Wheldon TE. Relationships between tumor size and curability for uniformly targeted therapy with beta-emitting radionuclides. *J Nucl Med* 1995;36:1902.
5. Kaminski MS, Zasadny KR, Francis IR, et al. Iodine-131-anti-B1 radioimmunotherapy for B-cell lymphoma. *J Clin Oncol* 1996;14:1974.
6. Witzig TE, Gordon LI, Cabanillas F, et al. Randomized, controlled trial of yttrium-90-labeled ibritumomab tiuxetan radioimmunotherapy versus rituximab immunotherapy for patients with relapsed or refractory low-grade, follicular, or transformed B-cell non-Hodgkin's lymphoma. *J Clin Oncol* 2002;20:2453.
7. Grillo-López AJ, Cheson BD, Horning SJ, et al. Response criteria for NHL: Importance of "normal" lymph node size and correlations with response rates. *Ann Oncol* 2000;11:399.
8. Kaminski MS, Tuck M, Estes J, et al. ^{131}I-tositumomab therapy as initial treatment for follicular lymphoma. *N Engl J Med* 2005;352:441.
9. Liu AY, Robinson RR, Murray ED, et al. Production of a mouse-human chimeric monoclonal antibody to CD20 with potent Fc-dependent biologic activity. *J Immunol* 1987;139:3521.
10. Leung S-O, Shevitz J, Pellegrini MC, et al. Chimerization of LL2, a rapidly internalizing antibody specific for B-cell lymphoma. *Hybridoma* 1994;13:469.
11. Howell RW. The MIRD schema: From organ to cellular dimensions. *J Nucl Med* 1994;35:531.
12. Loevinger R, Budinger TF, Watson EE. In: *MIRD Primer For Absorbed Dose Calculations.* New York: The Society of Nuclear Medicine, MIRD, 1991.
13. Griffiths GL, Govindan SV, Sgouros G, et al. Cytotoxicity with auger elctron-emitting radionuclides delivered by antibodies. *Int J Cancer* 1999;81:985.
14. Emfietzoglou D, Papamichael G, Kostarelos K, et al. A Monte Carlo track structure code for electrons (10 eV–10 keV) and protons (0.3–10 MeV) in water: Partitioning of energy and collision events. *Phys Med Biol* 2000;45:3171.
15. Emfietzoglou D, Karava K, Papamichael G, et al. Monte Carlo simulation of the energy loss of low-energy electrons in liquid water. *Phys Med Biol* 2003;48:2355.
16. Emfietzoglou D, Nikjoo H. The effect of model approximations on single-collision distributions of low-energy-electrons in liquid water. *Radiat Res* 2005; 163:98.
17. Emfietzoglou D, Cucinotta FA, Nikjoo H. A complete dielectric response model for liquid water—a solution of the Bethe ridge problem. *Radiat Res* 2005;164: 202.
18. Goddu SM, Howell RW, Bouchet LG, et al. MIRD Cellular S-values: Self-Absorbed Dose Per Unit Cumulated Activity for Selected Radionuclides and Monoenergetic Electron and Alpha Particle Emitters Incorporated Into Different Cell Compartments. Reston, VA: SNM, 1997.
19. Press OW, Fass J, Borroz KI, et al. Endocytosis and degradation of monoclonal antibodies targeting human B-cell malignancies. *Cancer Res* 1989;49:4906.
20. Hansen HJ, Ong GL, Diril H, et al. Internalization and catabolism of radiolabelled antibodies to the MHC class-II invariant chain by B-cell lymphomas. *Biochem J* 1996;320:293.
21. Stein R, Govindan SV, Mattes MJ, et al. Improved iodine radiolabels for monoclonal antibody therapy. *Cancer Res* 2003;63:111.

22. Govindan SV, Mattes MJ, Stein R, et al. Labeling of monoclonal antibodies with diethylenetriaminepentaacetic acid-appended radioiodinated peptides containing D-amino acids. *Bioconj Chem* 1999;10:231.
23. Hekman A, Honselaar A, Vuist WMJ, et al. Initial experience with treatment of human B-cell lymphoma with anti-CD19 monoclonal antibody. *Cancer Immunol Immunother* 1991;32:364.
24. Stabin MG, Siegel JA. Physical models and dose factors for use in internal dose assessment. *Health Phys* 2003;85:294.
25. Behr TM, Behe M, Lohr M, et al. Therapeutic advantages of Auger electron- over beta-emitting radiometals or radioiodine when conjugated to internalizing antibodies. *Eur J Nucl Med* 2000;27:753.
26. Griffiths GL, Govindan SV, Sgouros G, et al. Cytotoxicity with auger electron-emitting radionuclides delivered by antibodies. *Int J Can* 1999;81:985.
27. Ochakovskaya R, Osorio L, Goldenberg DM, et al. Therapy of disseminated B-cell lymphoma xenografts in severe combined immunodeficient mice with an anti-CD74 antibody conjugated with ^{111}Indium, ^{67}Gallium, or ^{90}Yttrium. *Clin Can Res* 2001;7:1505.
28. Welt S, Scott AM, Divgi CR, et al. Phase I/II study of iodine 125-labeled monoclonal antibody A33 in patients with advanced colon cancer. *J Clin Oncol* 1996;14:1787.
29. Du Y, Honeychurch J, Cragg MS, et al. Antibody-induced intracellular signaling works in combination with radiation to eradicate lymphoma in radioimmunotherapy. *Blood* 2004;103:1485.
30. Rossmann ED, Lundin J, Lenkei R, et al. Variability in B-cell antigen expression: Implications for the treatment of B-cell lymphomas and leukemias with monoclonal antibodies. *Hematol J* 2001;2:300.